Supplementary Information

Programmable Wavelength- and Time-Dependent Multicolor Afterglow in Polyvinyl Alcohol via Synergistic Ion-Bridging and Crosslinking Interactions

Shukang Yang,[a] Ying Lv,[a] Guorui Zhai,[a] Xiaohui Yu,[b] Jinmei Du,[a] Yang Jiang,[a] Dagang Miao,[a] Guowei Xiao,[a]* Changhai Xu[a]*

[a] College of Textiles & Clothing, Qingdao University, Qingdao, Shandong 266071, P. R. China.

[b] Jiangsu Lianfa textile Co, Ltd, Nantong, Jiangsu 226400, P. R. China.

Supplementary Methods

Experimental Procedures

Materials. Unless otherwise stated, all starting materials and reagents were purchased from commercial suppliers and used without further purification. All solvents were purified before use. The solvents were carefully dried and distilled from appropriate drying agents prior to use.

1.Material preparation method

The primary chemicals used in the experiments included type 1788 polyvinyl alcohol (PVA); 4-(bis(4-methoxyphenyl)amino)phenylboronic acid (purity 95%), denoted as 4-omPA; and NaCl (99.5%).

Under ambient conditions, PVA was employed as the luminescent matrix. First, 5 g of PVA was dissolved in 45 mL of deionized water under stirring in an oil bath at 88 °C until complete dissolution. Separately, 50 mg of the guest molecule 4-omPA was dissolved in 10 mL of anhydrous ethanol via ultrasonication until fully dissolved. The PVA solution was then cooled to 50 °C, after which the dissolved guest molecule was blended into the PVA solution under continued stirring until homogeneous mixing was achieved, yielding a PVA/4-omPA slurry. The slurry was cast onto a polytetrafluoroethylene (PTFE) mold and placed in an oven at 60 °C for 12 h to remove water and anhydrous ethanol, resulting in the fabrication of PVA/4-omPA films.

Similarly, under ambient conditions, 5 g of PVA along with 0.5 g of NaCl were dissolved in 45 mL of deionized water under stirring in an oil bath at 88 °C until fully dissolved. In parallel, 50 mg of 4-omPA was dissolved in 10 mL of anhydrous ethanol via ultrasonication. After cooling

the PVA/NaCl mixture to 50 °C, the dissolved guest molecule was incorporated and stirred until a uniform mixture was obtained, affording a PVA/4-omPA slurry. The slurry was cast onto a PTFE mold and dried in an oven at 60 °C for 12 h to eliminate water and ethanol, yielding the PVA/4-omPA@Na^+ films.

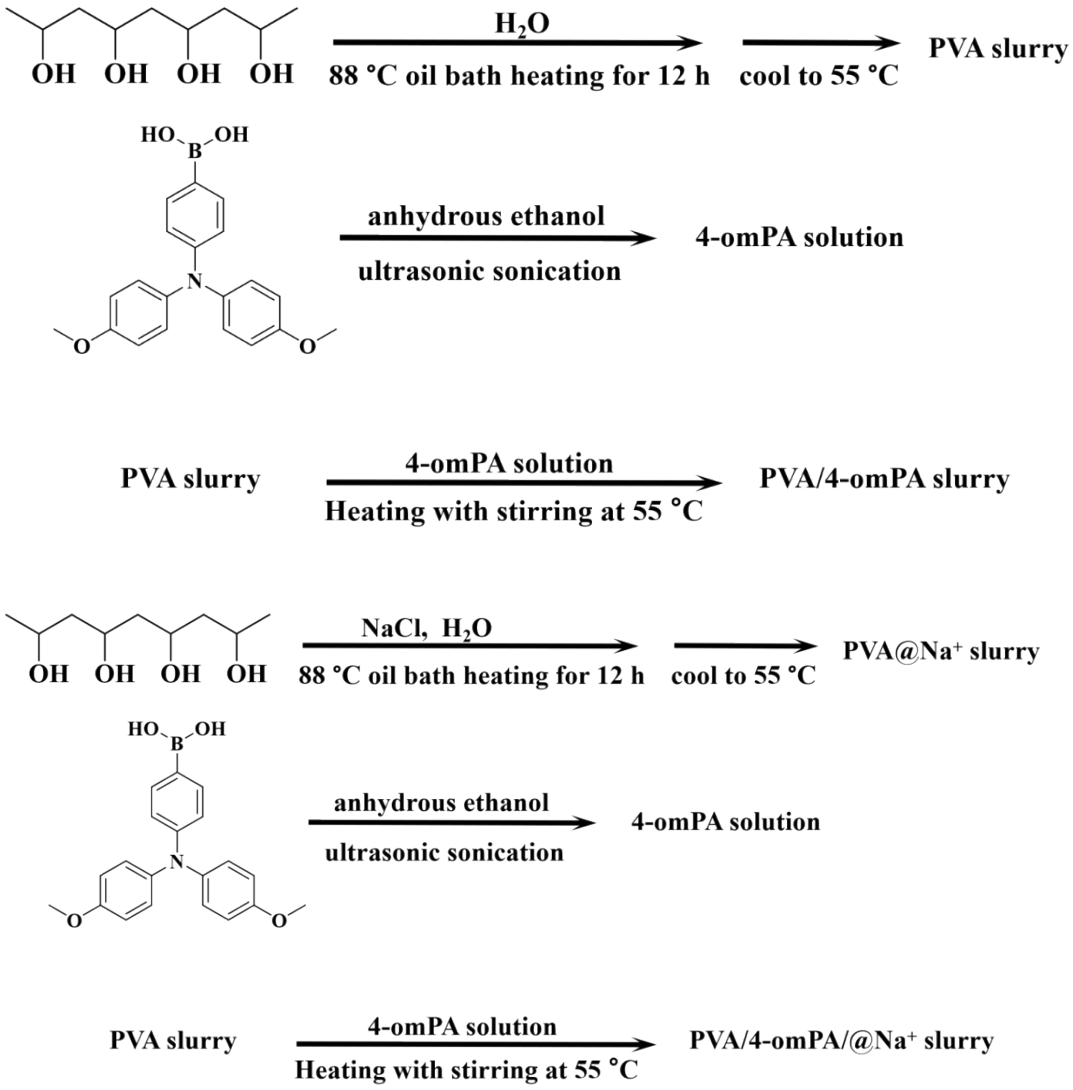

2.Electronic structure calculations of PVA/4-omPA@Na and PVA/4-omPA@Na^+.

All calculations were performed using density functional theory (DFT) as implemented in Gaussian 16 (Revision B.01).[50] Geometry optimizations were carried out using the B3LYP functional[51,52] with the def2-SVP basis set.[53] The Grimme D3 dispersion correction with Becke-Johnson damping (D3BJ) was included to account for dispersion interactions.[54] All structures were fully optimized without symmetry constraints.

The electrostatic potential (ESP) distributions, localized orbital locator-π (LOL-π), and frontier

molecular orbitals (HOMO and LUMO) were analyzed based on the optimized wavefunctions using Multiwfn.[55] The generated isosurfaces were visualized using VMD.[56]

3.Characterizations and instruments: Fluorescence spectra, phosphorescence spectra, and ultralong lifetimes were performed on the Edinburgh FLS1000.Excitation-fluorescence mapping and excitation-phosphorescence mapping were measured using Hitachi F-4700.X-ray Diffraction (XRD) data were measured using a Rigaku MiniFlex600 (Japan).Energy Dispersive X-ray Spectroscopy (EDS) and mapping data were measured using a Carl Zeiss Sigma 500 (Germany).The X-ray photoelectron spectroscopy (XPS) was obtained using a Shimadzu AXIS SUPRA+ spectrometer. Fourier transform infrared spectra (FT-IR) were recorded on the IRTracer-100.Differential Scanning Calorimetry-Thermogravimetric Analysis (DSC-TGA) data were measured using an SDT Q600 V8.3 Build 101. UV-vis absorption spectra were obtained on a PERSEE TU-1901 spectrophotometer. All films were photographed in a dark environment, at a temperature of 15–25 °C and a relative humidity of 40%–50%. The UV lamp used in the experiment was provided by InvaxCarDan, with model JY-88. The light source includes 365 nm UV and 395 nm UV, with a maximum power of 35 W.

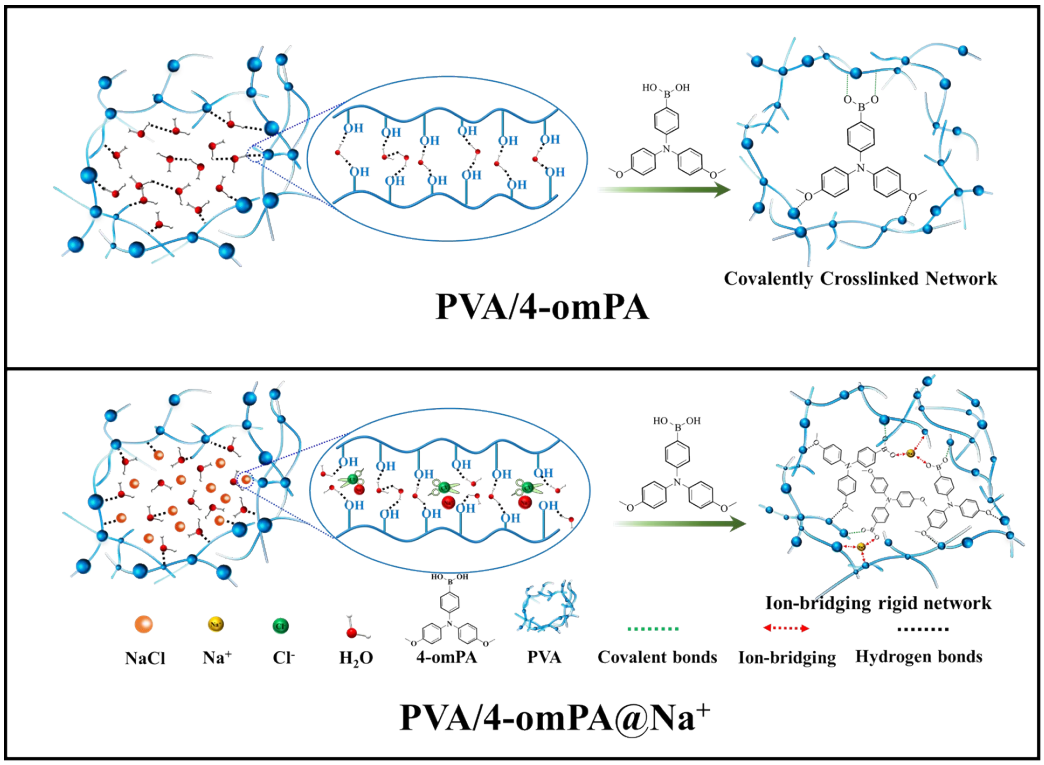

Fig. S1. Synthetic route and scheme of PVA/4-omPA and PVA/4-omPA@Na^+.

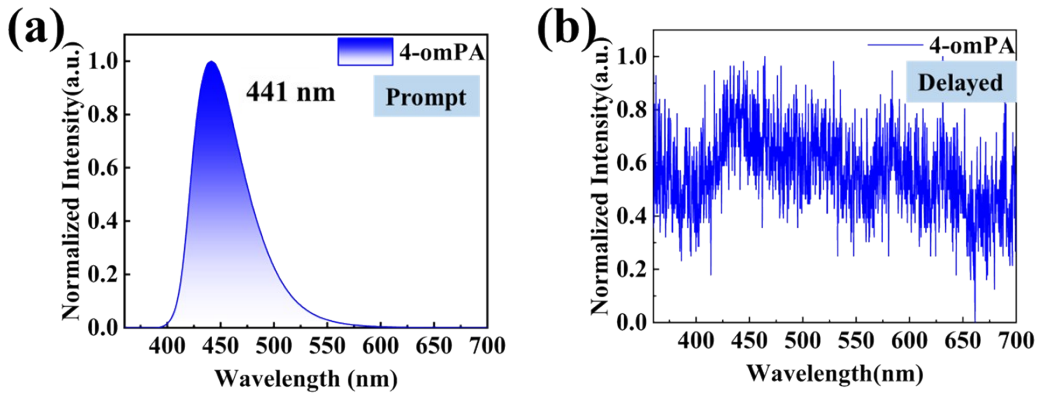

Fig. S2. (a, b) Fluorescence and phosphorescence spectra of 4-omPA.

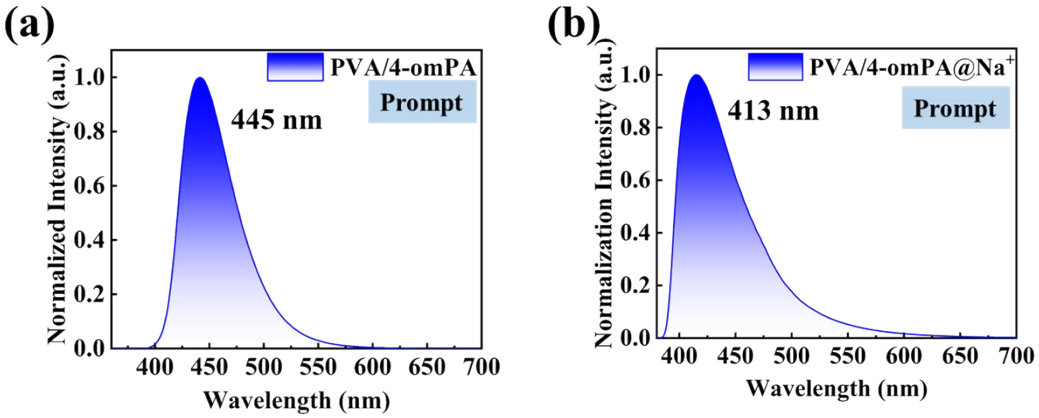

Fig. S3. (a, b) Fluorescence spectra of PVA/4-omPA and PVA/4-omPA@Na^+.

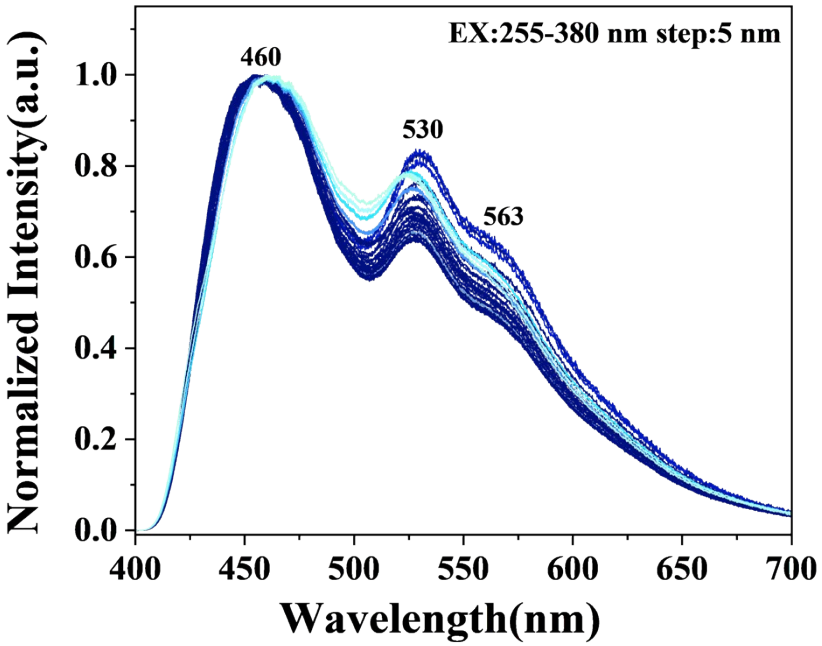

Fig. S4. Excitation (255 nm-380 nm)-phosphorescence mapping of PVA/4-omPA@Na^+ under ambient conditions.

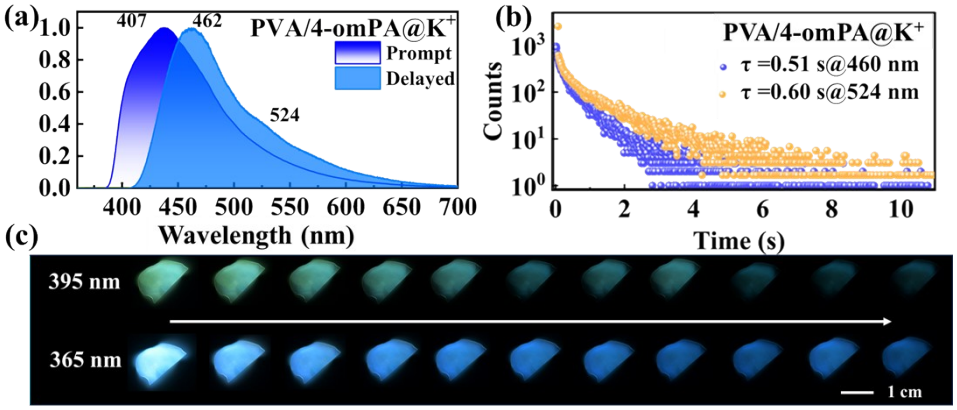

Fig. S5. (a-c) Fluorescence, phosphorescence spectra, time-resolved decay profiles and afterglow images of PVA/4-omPA@K^+.

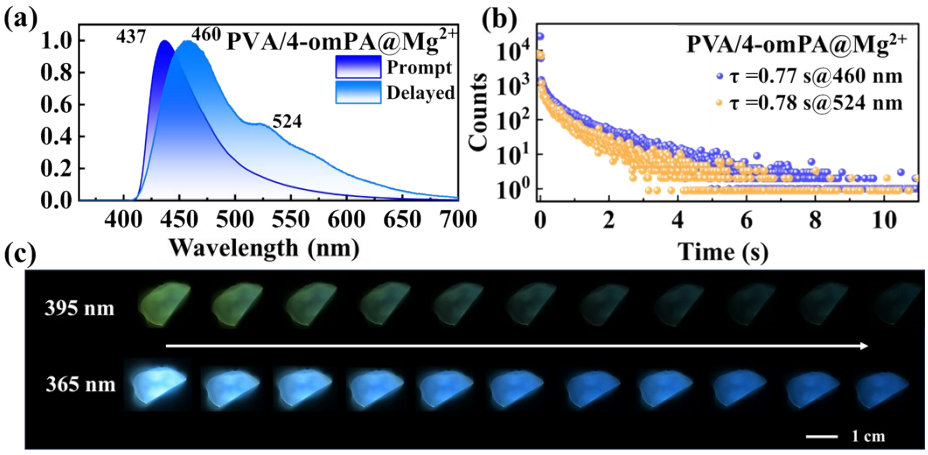

Fig. S6. (a-c) Fluorescence, phosphorescence spectra, time-resolved decay profiles and afterglow images of PVA/4-omPA@Mg^{2+}.

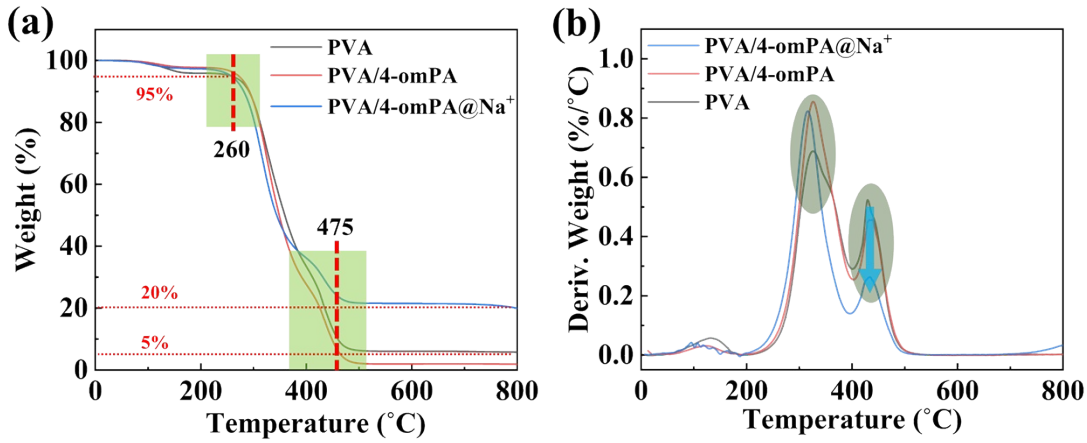

Fig. S7. (a,b) Thermogravimetric curves and weight loss rate curves of PVA, PVA/4-omPA, and PVA/4-omPA@Na^+, respectively.

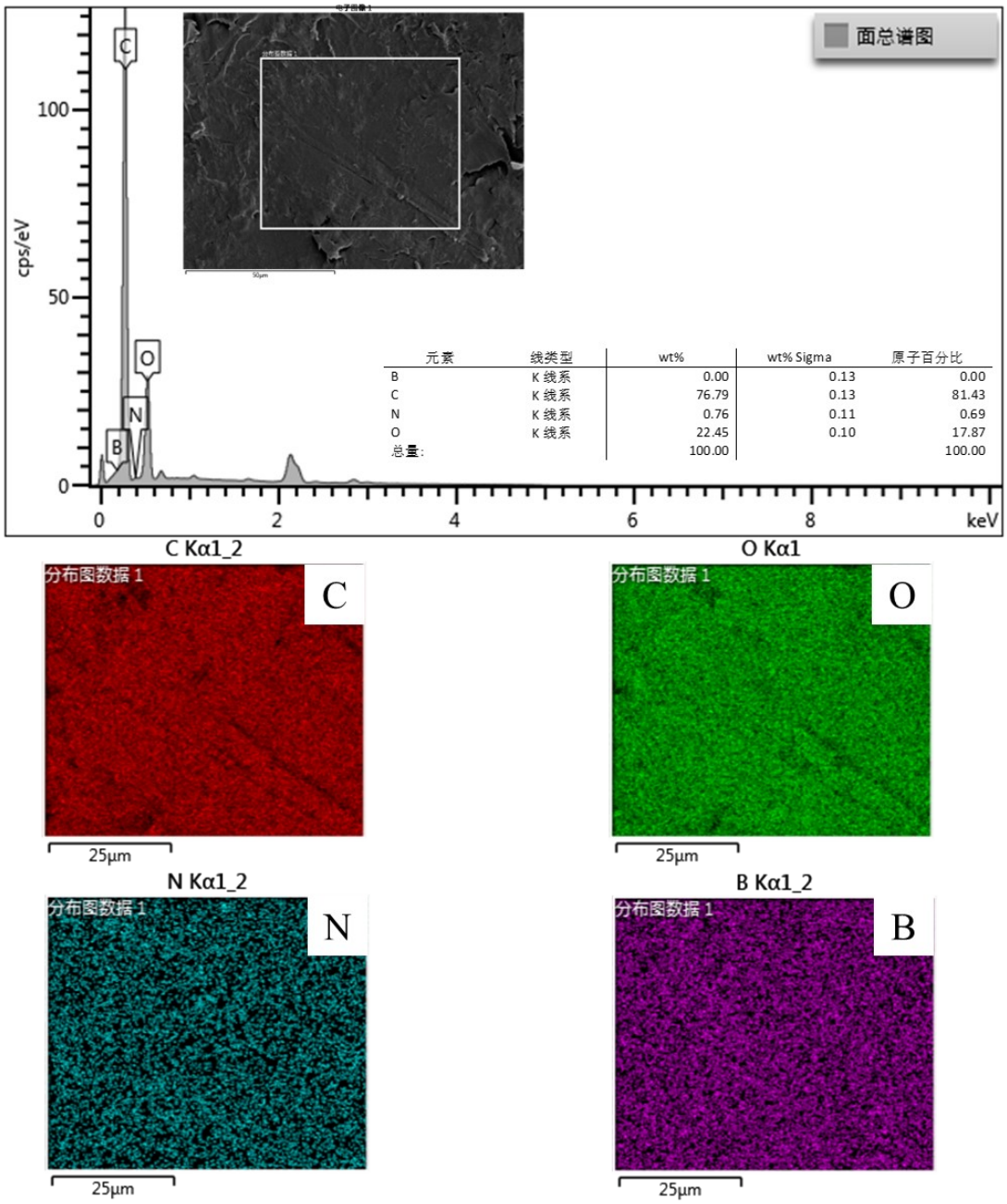

Fig. S8. EDS and elemental mapping of C, O, N and B in PVA/4-omPA.

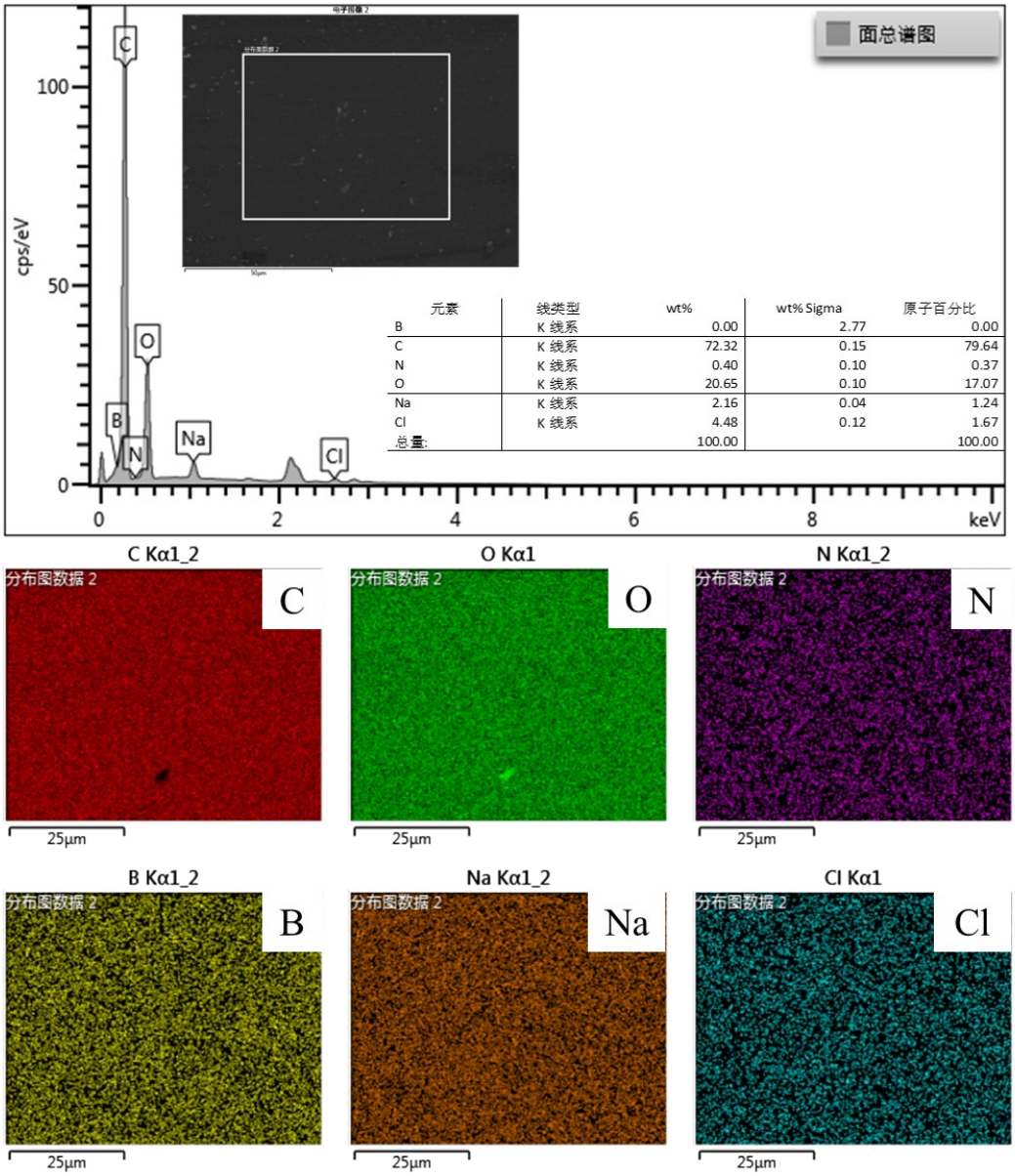

Fig. S9. EDS and elemental mapping of C, O, N, B, Na and Cl in PVA/4-omPA@Na^+.

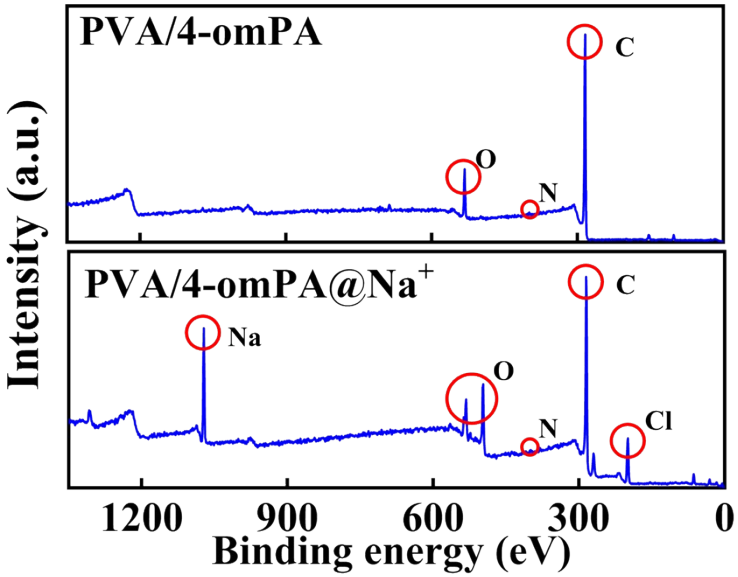

Fig. S10. XPS survey spectra of PVA/4-omPA and PVA/4-omPA@Na^+.

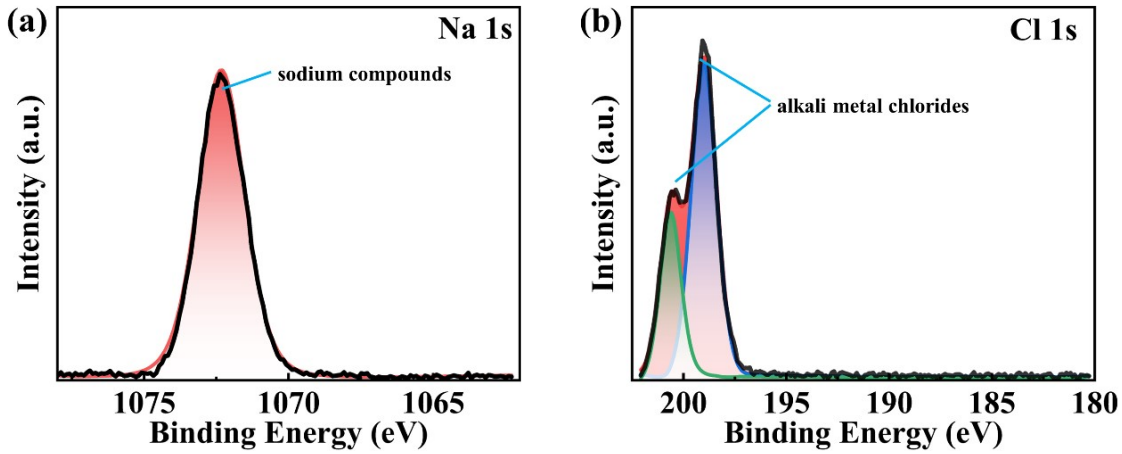

Fig. S11. Binding energies of Na and Cl elements in PVA/4-omPA@Na^+ from XPS measurements.

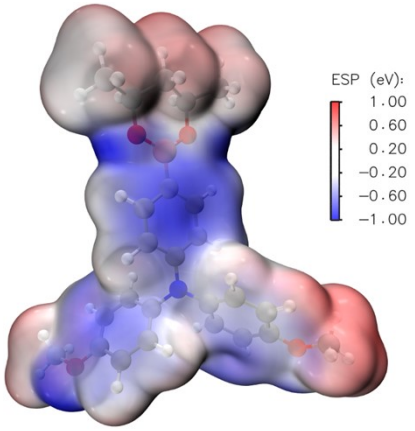

Fig. S12. The electrostatic potential (ESP) of PVA/4-omPA.

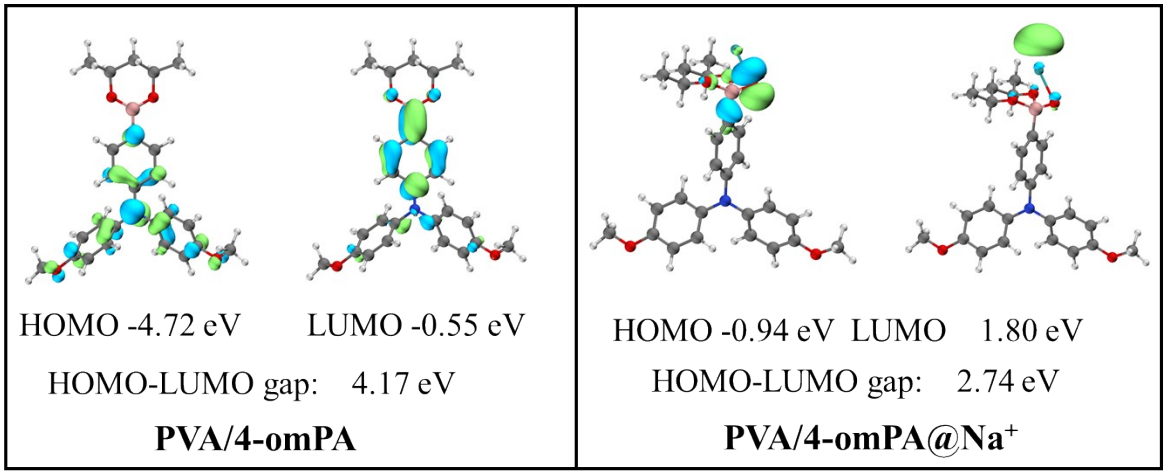

Fig. S13. The frontier molecular orbital distributions (HOMO and LUMO) of PVA/4-omPA and PVA/4-omPA@Na^+.

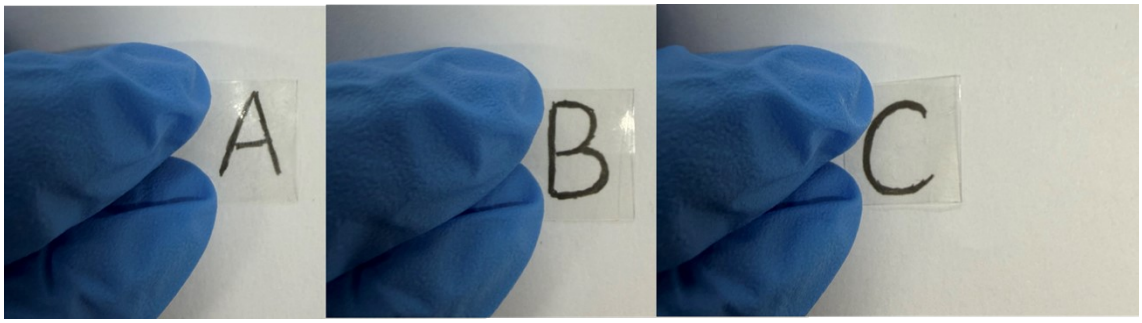

Fig. S14. Transparency of the three films: PVA, PVA/4-omPA, and PVA/4-omPA@Na^+.

Table S1 The fitting parameters for phosphorescence lifetimes.

Compound	λex (nm)	λem (nm)	τ_1 (ms)	A_1 (%)	τ_2 (ms)	A_2 (%)	<τ> (ms)	χ^2
PVA/4-omPA	280	460	738.9	41.95	1835	58.05	1375	1.3419
PVA/4-omPA@Na^+	250	460	307.2	23.39	1284	76.61	1055	1.0538
	250	530	238.4	37.48	1129	62.52	794	1.1194

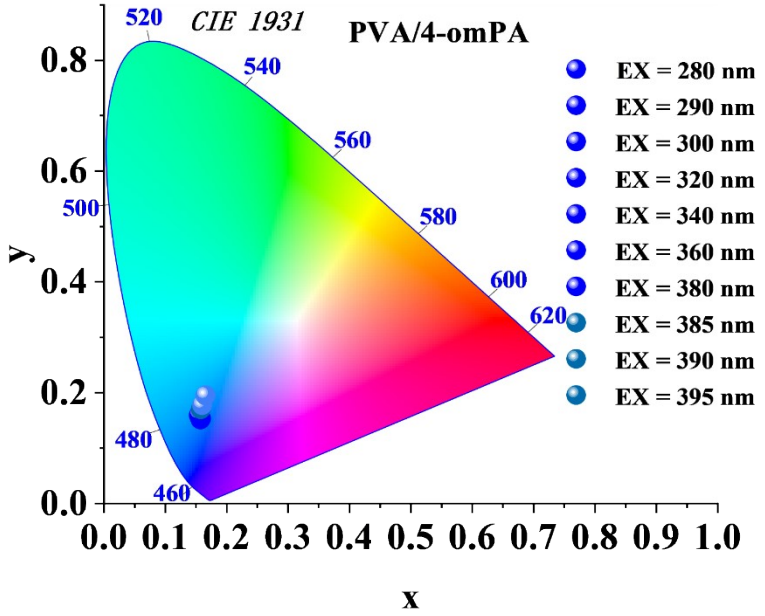

Table S2 CIE coordinate values of PVA/4-omPA under different excitations

λex (nm)	280	290	300	320	340	360	380	385	390	395
x	0.158	0.158	0.158	0.157	0.156	0.155	0.158	0.160	0.166	0.175
y	0.153	0.153	0.152	0.151	0.155	0.159	0.170	0.177	0.194	0.221

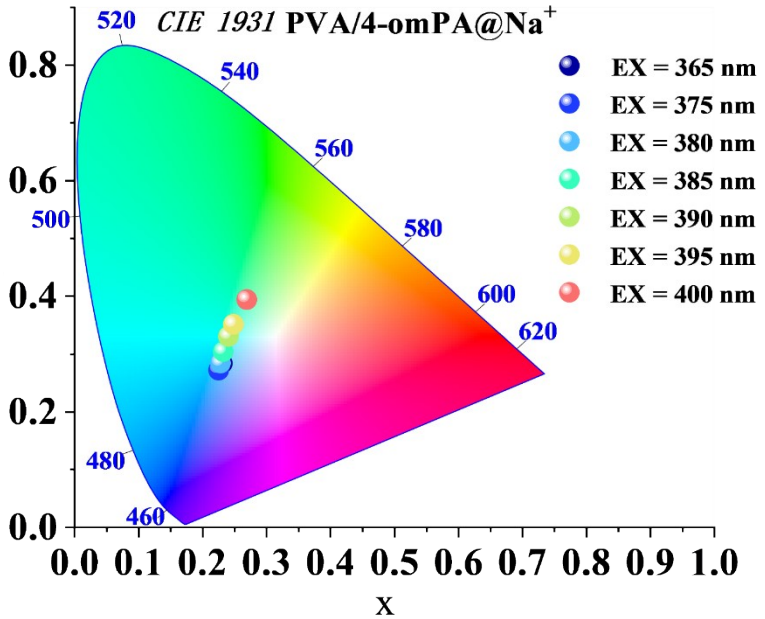

Table S3 CIE coordinate values of PVA/4-omPA@Na^+ under different excitations

λex (nm)	365	375	380	385	390	395	400
x	0.232	0.232	0.233	0.233	0.240	0.245	0.270
y	0.298	0.303	0.313	0.311	0.330	0.351	0.394

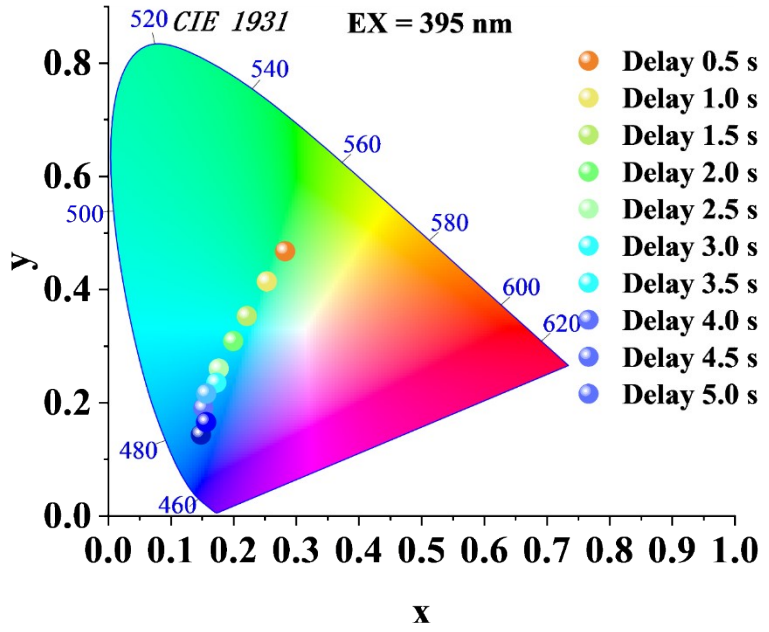

Table S4 CIE coordinate values of PVA/4-omPA@Na^+ at different delay time under 395 nm excitation

Delay (s)	0.5	1.0	1.5	2.0	2.5	3.0	3.5	4.0	4.5	5.0
x	0.282	0.253	0.221	0.199	0.176	0.172	0.156	0.152	0.156	0.148
y	0.467	0.412	0.353	0.308	0.260	0.235	0.216	0.190	0.165	0.143

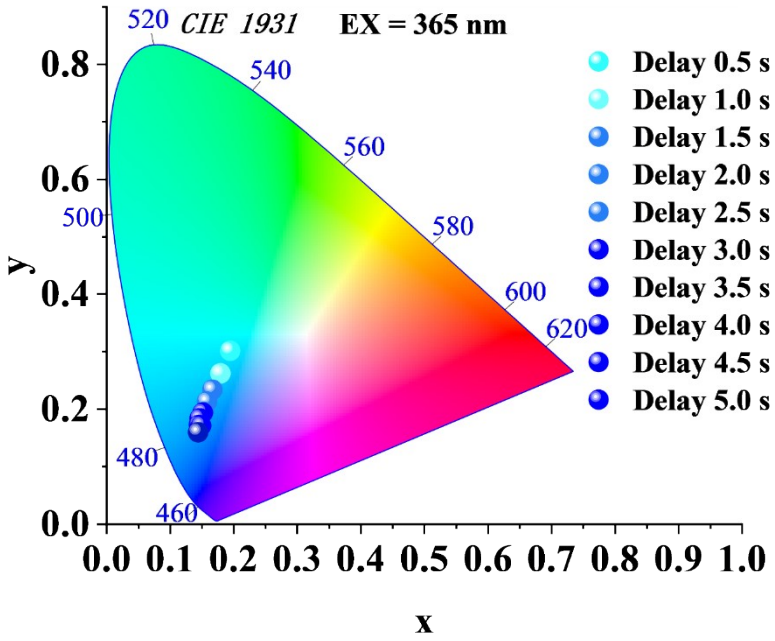

Table S5 CIE coordinate values of PVA/4-omPA@Na^+ at different delay time under 365 nm excitation

Delay (s)	0.5	1.0	1.5	2.0	2.5	3.0	3.5	4.0	4.5	5.0
x	0.194	0.176	0.166	0.158	0.153	0.151	0.146	0.145	0.149	0.144
y	0.301	0.262	0.233	0.212	0.195	0.194	0.183	0.172	0.171	0.160

References

50. M. J. Frisch, et al. Gaussian 16, Revision B.01; Gaussian Inc.: Wallingford CT, 2016.
51. A. D. Becke, J, Chem. Phys. 1993, **98**, 5648–5652.
52. C. Lee, W Yang, R. G. Parr, Phys. Rev. B 1988, **37**, 785–789.
53. F. Weigend, R. Ahlrichs, Phys. Chem. Chem. Phys. 2005, **7**, 3297–3305.
54. S. Grimme, S. Ehrlich, L. Goerigk, J. Comput. Chem. 2011, **32**, 1456–1465.
55. T. Lu, F Chen. J. Comput. Chem. 2012, **33**, 580–592.
56. W. Humphrey, A Dalke, K. Schulten, J. Mol. Graph. 1996, **14**, 33–38.